International Conference on Estuaries and Coasts
November 9-11, 2003, Hangzhou, China

2-D SUSPENDED SEDIMENT NUMERICAL SIMULATION OF THE OUJIANG ESTUARY

Mengguo LI
School of Civil Engineering, Tianjin University, Tianjin, 300072, China
Tianjin Research Institute of Water Transport Engineering, Tianjin, 300456, China.
E-mail: limengguo@sina.com

Chongren QIN
School of Civil Engineering, Tianjin University, Tianjin, 300072, China

Abstract: This paper develops a 2-D mathematical model system of suspended sediment movement under the combined action of wave and tidal flow, including an irregular wave transformation mathematical model, a tidal flow mathematical model under the action of wave and a suspended sediment transport model. A finite difference method is adopted for the wave model with rectangular grid, and for tidal flow model and sediment model with triangular grid. The model system is applied to simulate the suspended sediment movement of the Oujiang Estuary. Through simulation of three tidal processes, spring tide, moderate tide and neap tide, a good agreement between the computed data of suspended sediment concentration and the measured data of totally 52 synchronous gauging stations is found. The model system has been proven to be able to reproduce the suspended sediment field successfully.

Key words: Suspended sediment, Mathematical model, Tidal flow, The Oujiang Estuary

1. INTRODUCTION

The Oujiang River is the second largest river in Zhejiang province, China. In the estuary, there exit a chain of islands, and the underwater seabed topography is very complicated with shoals, sand barriers and channels interweaved together(See Fig.1). The hydrodynamics and sediment movement in the Oujiang River and its estuary are very complicated.

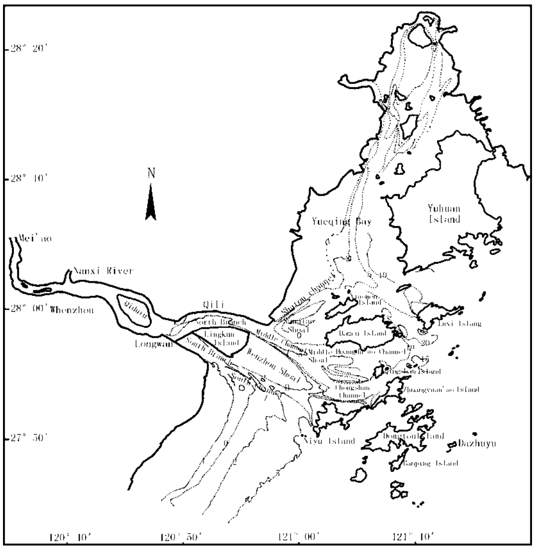

Fig. 1 Sketch of the Oujiang Estuary

To satisfy the need to develop Oujiang River and its estuary, it is necessary to have a detailed knowledge of the hydraulic conditions and sediment movement. Mathematical model is an economic and practical means in simulations of hydraulic forces and sediment movement.

This paper will develop a 2-D mathematical model system of suspended sediment movement caused by wave and tidal current, which includes an irregular wave transformation mathematical model (for calculating wave field), a tidal flow mathematical model taking into account wave through radiation stress and bed friction stress (for calculating current field), and a suspended sediment transport model taking into account wave through sediment-carrying capacity formula (for calculating suspended sediment field). A finite difference method is adopted for the wave model with rectangular grid, and a finite difference method is used for tidal current model and sediment model with triangular grid. The wave characteristics at triangular grid nodes are obtained from the rectangular grid nodes used by wave model through a linear interpolation method.

The model system will be used to numerically simulate the wave field, 2-D flow field and finally the suspended sediment field in the Oujiang River estuary.

2. MATHEMATICAL MODEL SYSTEM

2.1 WAVE MODEL

A multi-directional irregular wave transformation mathematical model developed by the author(Li Mengguo, 2001a, Li Mengguo and Liu Baiqiao, 2001) is adopted here. The model takes into account refractin, diffraction, breaking, bottom friction due to complex topography and islands comprehensively.

The present model has several advantages. Firstly, it is time-independent. It aims only at the calculation of wave direction and the distribution of wave energy, but not the depicting of wave surface undulation, so it avoids the difficulty in solving the potential function. Secondly, the present model can be numerically solved by finite difference method, having no limitations to the spatial step, and being able to be flexibly adjusted according to the calculation domain. Thirdly, it takes into account a number of factors affecting wave transformation, therefore, it is very suitable for the wave field computation of large coastal and estuarine waters with complex topography.

Finite difference scheme is used as numerical method and rectangular grid is adopted.

As the model is somewhat complicated and the space is limited, the governing equation and its numerical scheme are not given here. For details, please refer to Ref.(Li Mengguo and Liu Baiqiao, 2001).

2.2 TIDAL FLOW MODEL UNDER THE ACTION OF WAVE

2.2.1 Basic equations

Continuity equation

$$\frac{\partial \zeta}{\partial t}+\frac{\partial[(h+\zeta)u]}{\partial x}+\frac{\partial[(h+\zeta)v]}{\partial y}=0 \tag{1}$$

Momentum equation

$$\frac{\partial u}{\partial t}+u\frac{\partial u}{\partial x}+v\frac{\partial u}{\partial y}-fv=-g\frac{\partial \zeta}{\partial x}-\frac{\tau_x}{\rho(h+\zeta)}-\frac{1}{\rho(h+\zeta)}\left(\frac{\partial S_{xx}}{\partial x}+\frac{\partial S_{xy}}{\partial y}\right)+N_x\left(\frac{\partial^2 u}{\partial x^2}+\frac{\partial^2 u}{\partial y^2}\right) \tag{2}$$

$$\frac{\partial v}{\partial t}+u\frac{\partial v}{\partial x}+v\frac{\partial v}{\partial y}+fu=-g\frac{\partial \zeta}{\partial y}-\frac{\tau_y}{\rho(h+\zeta)}-\frac{1}{\rho(h+\zeta)}\left(\frac{\partial S_{yx}}{\partial x}+\frac{\partial S_{yy}}{\partial y}\right)+N_y\left(\frac{\partial^2 v}{\partial x^2}+\frac{\partial^2 v}{\partial y^2}\right) \tag{3}$$

where, x and y are the coordinates in the Cartesian coordinate system, in which xy plane coincides with still sea surface; u and v are depth-averaged velocity components in x and y directions respectively; g is acceleration due to gravity; ρ is water density; N_x and N_y are eddy viscosity coefficients of water in x and y directions respectively; t is time; and f is the Coriolis parameter; ζ is the water surface displacement relative to the xy plane; h is still water depth; S_{xx}, S_{xy}, S_{yx} and S_{yy} are four components of radiation stress of wave expressed as

$$S_{xx}=\frac{\rho g H^2}{8}\left[\left(2\frac{C_g}{C}-\frac{1}{2}\right)-\frac{C_g}{C}\sin^2\theta\right],\quad S_{xy}=S_{yx}=\frac{\rho g H^2}{8}\frac{C_g}{C}\sin\theta\cos\theta\ ,$$

$$S_{yy} = \frac{\rho g H^2}{8}\left[\left(\frac{C_g}{C} - \frac{1}{2}\right) + \frac{C_g}{C}\sin^2\theta\right]$$

in which, C_g , C , H and θ are wave group velocity, wave celerity, wave height and wave direction respectively;

τ_x and τ_y are bed resistance components in x and y directions respectively expressed as

$$\tau_x = \frac{g}{c^2}\rho\left|\vec{U}\right|u + \frac{\pi}{8}\rho f_w\left|\vec{U}_w\right|u_w + \frac{B\rho}{\pi}\sqrt{2}\left(\frac{gf_w}{c^2}\right)^{\frac{1}{2}}\left|\vec{U}\right|u_w \, . \; \tau_y = \frac{g}{c^2}\rho\left|\vec{U}\right|v + \frac{\pi}{8}\rho f_w\left|\vec{U}_w\right|v_w + \frac{B\rho}{\pi}\sqrt{2}\left(\frac{gf_w}{c^2}\right)^{\frac{1}{2}}\left|\vec{U}\right|v_w$$

in which, $\vec{U}$ is flow velocity vector, $\vec{U} = \sqrt{u^2 + v^2}$; $\vec{U}_w$ is the maximum water particle velocity vector on sea bed, $\vec{U}_w = \sqrt{u_w^2 + v_w^2}$, u_w and v_w being velocity components of $\vec{U}_w$ in x and y directions respectively; f_w is wave resistance coefficient on sea bed; c is Chezy coefficient, $c = (h+\zeta)^{1/6} / n$, n being Manning roughness coefficient; B is coefficient of wave and current interaction(Cao Zude, et al, 1993): $B = 0.917$ when wave and current are in the same direction, $B =$ -0.1983 when wave and current meet at right angles and $B = 0.359$ when included angle of wave and current is on other situations

If let $H = 0$, that is, the wave action is not taken into account, the model will reduce to tidal flow model only.

2.2.2 Boundary conditions

For the open boundary condition:

$$\zeta(x,y,t)\,|_{\Gamma_1} = \zeta^*(x,y,t)\ , \text{ or } \left.\begin{aligned} u(x,y,t)\,|_{\Gamma_1} &= u^*(x,y,t) \\ v(x,y,t)\,|_{\Gamma_1} &= v^*(x,y,t) \end{aligned}\right\}$$

in which Γ_1 expresses open boundary; subscript * expresses a given value(the measured value or analyzed value).

For the closed boundary condition

$$\vec{U}\cdot\vec{n}\Big|_{\Gamma 2} = 0$$

in which, Γ_2 expresses closed boundary; $\vec{n}$ expresses normal unit vector.

2.2.3 Initial condition

$$\left.\begin{aligned} \zeta(x,y,t)\big|_{t=0} &= \zeta_0(x,y) \\ u(x,y,t)\big|_{t=0} &= u_0(x,y) \\ v(x,y,t)\big|_{t=0} &= v_0(x,y) \end{aligned}\right\}$$

where subscript 0 expresses a given value(the measured value or analyzed value).

2.2.4 Numerical method

A second-order explicit finite difference numerical method with triangular grid(Li Mengguo and Wang Zhenglin,2002)is used. The difference equations are as follows(the detailed derivations are presented in Ref.(Li Mengguo, 2001b; Li Mengguo and Wang Zhenglin,2002)).

$$\zeta_M^{K+1} = \zeta_M^K - \left(\frac{\partial}{\partial x}\left\{(h+\zeta^K)u^K\Delta t + \left[(h+\zeta^K)\left(\frac{\partial u}{\partial t}\right)^K + \left(\frac{\partial \zeta}{\partial t}\right)^K u^K\right]\frac{(\Delta t)^2}{2}\right\}\right)_M^K$$
$$- \left(\frac{\partial}{\partial y}\left\{(h+\zeta^K)v^K\Delta t + \left[(h+\zeta^K)\left(\frac{\partial v}{\partial t}\right)^K + \left(\frac{\partial \zeta}{\partial t}\right)^K v^K\right]\frac{(\Delta t)^2}{2}\right\}\right)_M^K \tag{4}$$

$$u_M^{K+1} = \frac{C_1 \times B_1 - C_2 \times B_1}{A_1 \times B_2 - A_2 \times B_1} \tag{5}$$

$$v_M^{K+1}=\frac{A_1\times C_2-A_2\times C_1}{A_1\times B_2-A_2\times B_1} \tag{6}$$

In the above, M is the number of nodal point; K is the number of time steps; Δt is the step of time; expressions of $A_1\ B_1\ C_1\ A_2\ B_2\ C_2$ are as follows:

$$A_1=\frac{2}{\Delta t}+\left(\frac{\partial u}{\partial x}\right)_M^K+\frac{g\sqrt{(u_M^K)^2+(v_M^K)^2}}{(h_M+\zeta_M^{K+1})(c_M^{K+1})^2}\,,\quad B_1=\left(\frac{\partial v}{\partial y}\right)_M^K-f$$

$$C_1=\frac{2}{\Delta t}u_M^K+\left(\frac{\partial u}{\partial t}\right)_M^K-g\left(\frac{\partial \zeta}{\partial x}\right)_M^{K+1}+N_x\left(\frac{\partial^2 u}{\partial x^2}+\frac{\partial^2 u}{\partial y^2}\right)_M^K-\frac{1}{(h_M+\zeta_M^{K+1})}\left(\frac{\partial S_{xx}}{\partial x}+\frac{\partial S_{xy}}{\partial y}\right)_M^K$$

$$-\frac{1}{(h_M+\zeta_{Mi}^{K+1})}\left[\frac{\pi}{8}(f_w|\vec{U}_w|u_w)+\frac{B\sqrt{2f_w g(u^2+v^2)}}{\pi c}u_w\right]_M^K,$$

$$A_2=\left(\frac{\partial v}{\partial x}\right)_i^K+f\,,\quad B_2=\frac{2}{\Delta t}+\left(\frac{\partial v}{\partial y}\right)_M^K+\frac{g\sqrt{(u_M^K)^2+(v_M^K)^2}}{(h_M+\zeta_{Mi}^{K+1})(c_M^{K+1})^2},$$

$$C_2=\frac{2}{\Delta t}v_M^K+\left(\frac{\partial v}{\partial t}\right)_M^K-g\left(\frac{\partial \zeta}{\partial y}\right)_M^{K+1}+N_y\left(\frac{\partial^2 v}{\partial x^2}+\frac{\partial^2 v}{\partial y^2}\right)_M^K-\frac{1}{(h_M+\zeta_{Mi}^{K+1})}\left(\frac{\partial S_{yx}}{\partial x}+\frac{\partial S_{yy}}{\partial y}\right)_M^K$$

$$-\frac{1}{h_M+\zeta_M^{K+1}}\left[\frac{\pi}{8}(f_w|\vec{U}_w|v_w)+\frac{B\sqrt{2f_w g(u^2+v^2)}}{\pi c}v_w\right]_M^K$$

2.2.5 Determination method of wave characteristics at triangular grid nodes

As the wave model and the tidal flow model under the action of wave use different grids, the wave characteristics at triangular grid nodes have to be obtained from those at rectangular grid nodes by interpolation. A linear interpolation method is used in this paper.

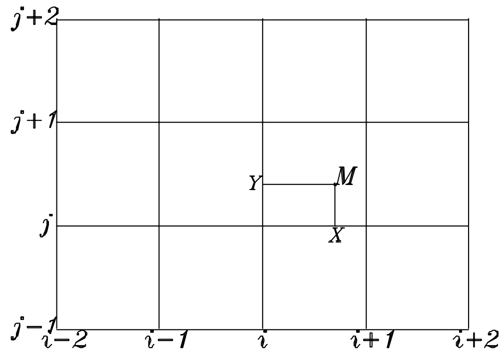

Fig. 2 Sketch of a triangular grid node in rectangular grid

Given F stands for arbitrary one of wave height H and wave direction θ, and given F_M stands for value of F at some triangular grid node M located in rectangular grid system(See Fig.2), then

$$F_M=(1-X)(1-Y)F_{i,j}+X(1-Y)F_{i+1,j}+(1-X)YF_{i,j+1}+XYF_{i+1,j+1} \tag{7}$$

in which, $F_{i,j}$, $F_{i+1,j}$, $F_{i,j+1}$, $F_{i+1,j+1}$ are values of F at rectangular grid nodes(i,j), ($i+1,j$), ($i,j+1$), ($i+1,j+1$) respectively; X and Y are ratios of coordinates of M in local coordinate system with (i,j) as its origin to spatial step Δx and Δy respectively, ranging from 0 to 1.

2.3 SUSPENDED SEDIMENT MODEL

2.3.1 Basic equations

$$\frac{\partial[(h+\zeta)S]}{\partial t}+\frac{\partial[(h+\zeta)uS]}{\partial x}+\frac{\partial[(h+\zeta)vS]}{\partial y}+\alpha\omega(S-S_*)=\frac{\partial}{\partial x}\left[(h+\zeta)D_x\frac{\partial S}{\partial x}\right]+\frac{\partial}{\partial y}\left[(h+\zeta)D_y\frac{\partial S}{\partial y}\right] \tag{8}$$

in which, S is depth-averaged suspended sediment content; D_x and D_y are diffusion coefficients of suspended sediment in x and y directions respectively; α is the settlement rate of suspended sediment; ω is the settling velocity of suspended sediment; S_* is the sediment-carrying capacity of current.

2.3.2 Boundary conditions

For the open boundary conditions:

Inflow: $S(x,y,t)|_{\Gamma_1} = S^*(x,y,t)$

Outflow: $\frac{\partial(h+\zeta)S}{\partial t} + \frac{\partial(h+\zeta)Su}{\partial x} + \frac{\partial(h+\zeta)Sv}{\partial y} = 0$

In which, subscript * expresses a given value(the measured value or analyzed value); Γ_1 expresses open boundary.

For the closed boundary condition: $\left.\frac{\partial S}{\partial \vec{n}}\right|_{\Gamma_2}$ =0

where Γ_2 expresses closed boundary.

2.3.3 Initial condition

$$S(x,y,t)\big|_{t=0} = S_0(x,y)$$

where subscript 0 expresses a given value(the measured value or analyzed value).

2.3.4 Numerical method

Explicit finite difference numerical method is used, and the numerical difference equation is as follows:

$$S_M^{K+1} = S_M^K - \Delta t\left(u_M^K\left(\frac{\partial S}{\partial x}\right)_M^K + v_M^K\left(\frac{\partial S}{\partial y}\right)_M^K\right) + \Delta t\left(D_x\left(\frac{\partial^2 S}{\partial x^2}\right)_M^K + D_y\left(\frac{\partial^2 S}{\partial y^2}\right)_M^K\right)$$

$$\frac{\Delta t}{h_M+\zeta_M^{K+1}}\left(\frac{\partial[D_x(h+\zeta)]}{\partial x}\right)_M^K\left(\frac{\partial S}{\partial x}\right)_M^K + \frac{\Delta t}{h_M+\zeta_M^{K+1}}\left(\frac{\partial[D_y(h+\zeta)]}{\partial y}\right)_M^K\left(\frac{\partial S}{\partial x}\right)_M^K - \frac{\Delta t[\alpha(S-S_*)]_M^K}{h_M+\zeta_M^{K+1}} \quad (9)$$

where the first-order spatial partial derivatives are treated by "upwind" scheme(Li Mengguo, 2001b).

3. DETERMINATION OF COMPUTATION DOMAIN AND DIVISION OF GRIDS

3.1 WAVE COMPUTATION DOMAIN AND GRID DIVISION

As there is a long-term wave observation station at Nanji Island, according to the practical need to solve the problem, the wave computation domain is chosen. The west boundary reaches 120°30'E, and the east boundary reaches 121°45'E. The north boundary reaches the head of Yueqing Bay, and the south boundary reaches 27°10'N. It is about 125km wide in the east-west direction and about 133km long in the south-north direction. There are many islands in the computation domain, such as the island chain outside the Oujiang Estuary , Nanji Island, etc. The computation domain includes three estuaries, the Oujiang Estuary, the Feiyunjiang Estuary and the Aojiang Estuary. For details, please refer to Ref.(Li Mengguo and Liu Baiqiao, 2001).

Square grid (a special kind of rectangular grid) is adopted to divide the computation domain. There are 1000×1068 grid nodes in the domain, the nodal interval being 125m.

Fig. 3 Triangular grid of the Oujiang

3.2 TIDAL FLOW AND SUSPENDED SEDIMENT COMPUTATION DOMAIN AND GRID DIVISION

The computation domain is shown in Fig.1. The west boundary reaches Mei'ao, and the east boundary reaches 121°20'E. The north boundary reaches the head of Yueqing Bay, and the south boundary reaches 27°44'N. It is about 72.2km long in the east-west direction and about 71.5km wide in the south-north direction. There are 43 islands being taken into account in the computation domain.

Irregular triangular grid is adopted to divide the computation domain(See Fig.3). There are 33606 triangular grid nodes and 64614 triangular elements in the domain. The minimum spatial step is 30m and the maximum spatial step is 800m.

4. DETERMINATIONS OF SOME IMPORTANT PARAMETERS

There are a few parameters in the mathematical system that must be determined reasonably before the model system is operated. The determination of the parameters will be given in the following.

(1) Manning roughness coefficient n

n is in the range of 0.010－0.025.

(2) N_x, N_y, D_x, D_y

N_x, N_y, D_x and D_y are taken according to Ref.(Wu Yixi and Cao Zude,1999).

(3) ω

Most coasts and estuaries in China are of silt sandy coast, and the particle size of suspended sediment is fine with a little variation. The sediment settles and is transported in a form of flocculated mass under the action of saltine water. Tests shows that the particle size of the flocculated equivalent is about in the range of 0.015－0.03mm, and the corresponding settling velocity is in the range of 0.01－0.06cm/s. In this study, ω takes 0.04cm/s.

(4) sediment-carrying capacity S_*

Sediment-carrying capacity is a very important parameter in suspended sediment simulation. According to the analysis of field data, the following expression is gained

$$S_* = \beta \frac{(\sqrt{u^2 + v^2} + \gamma U_w)^3}{g(h+\zeta)\omega}$$

where, β is settling probability, in this study, β=0.08755; γ is an empirical coefficient determined by field data.

5. NUMERICAL SIMULATIONS

The developed mathematical system has been applied to the simulations of the Oujiang Estuary.

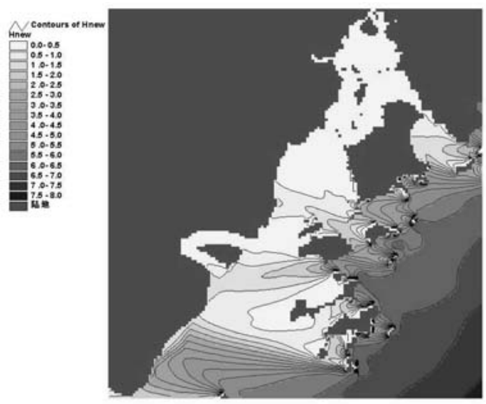

Fig. 4 Computed wave field at high slack water I in the Oujiang Estuary

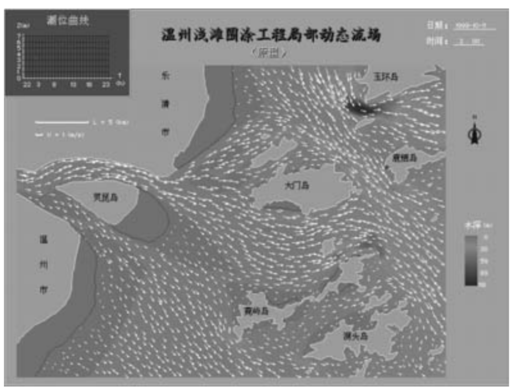

Fig. 5 Computed flow field at fall strength in the Oujiang Estuary

The wave model has been applied to compute wave field of different water levels due to incident wave from out sea. Wave fileds of the incident waves from NNE, NE, ENE, E, ESE, SE, SSE and S have been computed. Fig.4 is a computed wave field at high slack water, in which, the direction of the incident wave is E; the wave period is 7.4s and the wave height at Nanji Island is 7.5m. For other computation results, please refer to Ref.(Li Mengguo, 2001a).

The tidal flow model has been applied to simulate tidal flow field of the Oujiang Estuary, and the suspended sediment model has been applied to simulate the suspended sediment field by tidal flow and by both tidal flow and wave.

There are three times of synchronous hydrometric measurement conducted in the Oujiang Estuary. The first (spring tide) was conducted from Oct.10 to 12, 1999, the second (moderate tide)from Oct. 12 to 13,1999, and the third from Oct. 14 to 15,1999. There are 16 tidal level observation stations in each measurement, and there are 15, 19, 18 gauging stations in the first, second and third measurement respectively, where flow velocity, flow direction and suspended sediment content are observed. Through simulations of the three tidal processes, good agreement is found between computed data and observed data in both magnitude and phase. As the space is limited, the verification hydrographs are not given here. Fig.5 is the computed tidal flow field, and Fig.6 is the computed suspended sediment field.

Fig. 6 Suspended sediment field at low slack water

It can be seen from Fig.7 and Fig.8 that difference exists in the computed suspended sediment field with and without the action of wave. According to remote sensing analysis of suspended sediment distribution(Wen Lingping, 2001), there is a general law that the suspended sediment content in nearshore shallow water is higher that in offshore deep water, so the suspended sediment distribution in Fig.8 is more reasonable than in Fig.7, that is, the sediment-lifting role played by wave should be taken into account.

Fig. 7 Suspended sediment field transported by tidal flow at some time

Fig. 8 Suspended sediment field transported by tidal flow and wave at some time

6. CONCLUSIONS

A 2-D mathematical model system of suspended sediment movement has been set up, which consists of an irregular wave transformation model, a tidal flow model under the action of wave and a suspended sediment movement model. The model system has been successfully applied to the simulations of the Oujiang Estuary, and the wave field, flow field and suspended sediment field has been successfully reproduced. Simulation shows that wave and tidal flow should all be taken into account to simulate practical suspended sediment movement well. The model has no restrictions on the sea areas and can be popularized and widely used in numerical simulations of wave field, tidal flow field and suspended sediment movement in coastal and estuarine waters.

REFERENCES

Cao Zude and Wang Guifen, 1993. Numerical simulation of sediment lifted by wave and transported by tidal current. *Acta Oceanologica Sinica.* Vol.15, No.1,107-118(In Chinese).

Li Mengguo, 2001a. Technical report of mathematical modeling on wave in the Oujiang Estuary. Tianjin Research Institute of Water Transport Engineering(In Chinese).

Li Mengguo and Liu Baiqiao, 2001. Numerical study on the wave field in Oujiang Estuary. *Journal of Waterway and Harbor* No.1, pp1-8(In Chinese).

Li Mengguo, 2001b. Technical report of mathematical modeling on tidal flow, salinity, and sediment for the Reclamation Project of Whenzhou Shoal. Tianjin Research Institute of Water Transport Engineering(In Chinese).

Li Mengguo and Wang Zhenglin, 2002. Tidal flow numerical simulation of the Oujiang Estuary. *Journal of Yangtze River Scientific Research Institute*. Vol.29,No.2, pp19-22.(In Chinese).

Wu Yixi and Cao zude, 1999. Technical Regulations of Modeling for Tide-current and Sediment on Coast and Estuary. Beijing, Renmin Jiaotong Press(in Chinese).

Wen Lingping, 2001. Technical report of remote sensing analysis on suspended sediment distribution and its transport and deposition for the reclamation project of the Wenzhou Shoal. Tianjin Research Institute of Water Transport Engineering(in Chinese).